PAPER • OPEN ACCESS

Surface modification of tungsten carbide cobalt by electrical discharge coating with quarry dust powder: an optimisation study

View the article online for updates and enhancements.

Materials Research Express

PAPER

Surface modification of tungsten carbide cobalt by electrical discharge coating with quarry dust powder: an optimisation study

Ching Yee Yap[1] , Pay Jun Liew[1] and Jingsi Wang[2]

[1] Faculty of Manufacturing Engineering, Universiti Teknikal Malaysia Melaka, Hang Tuah Jaya, 76100 Durian Tunggal, Melaka, Malaysia
[2] Marine Engineering College, Dalian Maritime University, 1 Linghai Road, Ganjingzi District, Dalian 116026, People's Republic of China

E-mail: payjun@utem.edu.my

Abstract

In this paper, quarry dust was reused as a coating material on tungsten carbide cobalt (WC–Co) via electrical discharge coating (EDC). Before the EDC process, the quarry dust was mixed well with low smell kerosene oil and surfactant Span 85 to produce a new formulation of dielectric fluid. Response surface methodology was used to investigate the effect of EDC parameters, namely peak current (I_p, 3–5 A) and pulse on time (T_{on}, 100–300 μs) on the characteristics of the coating surface, including its Vickers micro-hardness, surface roughness and coating layer thickness. Results showed that an increment in I_p and T_{on} increased the Vickers micro-hardness and coating layer thickness yet decreased the surface finish. The optimum parameters for achieving a hard surface, thick coating layer and low surface roughness are $I_p = 4$ A and $T_{on} = 341$ μs. The established RSM model was in reasonable agreement with the experimental outcomes, and these findings could be useful in the cutting tools, moulds and dies industries for surface modification purposes.

1. Introduction

Tungsten carbide (WC) is a metal ceramic composite. It has a hard phase and hexagonal crystal structure. WC comprises a cobalt (Co) binder to form WC–Co as the Co content increases the fracture toughness and wear resistance [1, 2]. With its great technological and industrial importance, WC–Co has been widely used in many industrial applications, including as cutting tools, dies and moulds [1]. However, WC–Co has a short service life due to the formation of microcracks on the machined surface [3]. Therefore, a surface modification of WC–Co via hard material coating is deemed necessary to enhance its surface quality and to prevent the formation of microcracks.

The past century has witnessed a dramatic increase in the need for surface modification to enhance the physical, chemical or biochemical properties of materials, including their hardness, roughness, wear, corrosion and thermal resistance [4, 5]. Surface modification is also employed in industries to enhance the lifespan of products and to reduce the cost of tooling and moulding [6]. Many researchers are facing challenges from the rising demand for high-precision components with fine surface roughness and high wear and corrosion resistance [7]. Therefore, electrical discharge coating (EDC) via conventional electrical discharge machines has been proposed to improve the surface integrity of materials [7, 8]. EDC is a revolutionary surface modification process. By changing the suitable electrode polarity and dielectric fluid of the conventional EDM process, EDC process able to improve the physical, mechanical and biochemical properties of materials [9, 10]. Adding a suitable fine powder to the dielectric fluid during the EDC process may reduce the dielectric strength and increase the gap distance between the electrode and workpiece surface, thereby enhancing surface modification efficiency [11, 12]. According to Sharma *et al* [13], during the EDC process, the suspended powder tries to form a conductive bridge in the sparking gap under the influence of an electric field. When the gap resistance is reduced, an electrical spark will take place. The temperature during the electric spark is extremely high and usually ranges from 8000 °C to 12000 °C. Under this high temperature, the suspended powder and workpiece material are

simultaneously melted, and some of the molten elements are ejected from the workpiece and suspended powder. However, the flushing pressure resulting from the collapse of vapor bubbles is not sufficient to remove all molten materials [14]. Therefore, these molten elements migrate and are solidified on the workpiece surface via a rapid cooling process (quenching). After the EDC process, an extremely hard recast layer comprising an inter-mixture of molten materials from the workpiece, tool electrode and dielectric fluid may be created [15].

A growing number of studies have highlighted the importance of surface modification in increasing the strength, wear resistance and corrosion resistance of material surfaces. For example, Mohanty *et al* [14] performed a surface modification of titanium (Ti)–alloy by using WS_2 powder suspension and found that a coated surface with low specific wear rate and high hardness (881.34 HV) can be achieved via EDC. Tyagi *et al* [16] argued that a surface coated with tungsten disulphide (WS_2)- and copper (Cu)-mixed electrode via EDC has a lower wear value (6.71 μm) than the original workpiece (95.75 μm). Philip *et al* [17] found that the continuous squashing and sintering nature of EDC can produce a coated layer on the surface of the Ti6Al4V workpiece with superior wear resistance and ceramic characteristics. Philip *et al* [18] claimed that the protective tribo-oxides (TiO_2 and Ti_8O_{15}) and hard carbide ($Ti_{24}C_{15}$) in the recast layer, which are produced via EDC, can improve the tribology performance of the Ti6Al4V workpiece. Yu *et al* [19] discovered that Ti has a higher surface hardness and corrosion resistance after undergoing EDC with gas-assisted perforated (rotation) electrodes. Nonetheless, EDC is not truly free from pollution given that the use of dielectric fluids may generate some by-products [5]. Moreover, the cost effectiveness and lifetime of EDC process are difficult to determine. For instance, to maintain a constant amount of powder in dielectric fluid is difficult [20]. Therefore, the long-term efficiency and environmental impact of EDC required further investigation.

Several researchers have investigated the parametric optimisation of EDC for surface modification purposes. For example, Rahang and Patowari [21] used ANOVA and the Taguchi method to evaluate the use of EDC (in terms of tool wear rate, material transfer rate, surface roughness and edge deviation) in coating an aluminium surface with tungsten-copper (W–Cu) metallurgical green compact electrode. Chakraborty *et al* [22] applied signal-to-noise (S/N) ratio ANOVA to investigate the effect of peak current (I_p), pulse on time (T_{on}), electrode compact load and electrode composition on the coating of Al-6351 alloy surface with the green compact silicon carbide-copper (SiC-Cu) electrode. Vijayakumar *et al* [23] examined the mass loss on the coated surface of aluminium alloy 7075 when conducting EDC with nickel–silicon carbide (Ni–SiC)-powder-mixed dielectric fluid. Bhattacharya *et al* [24] used Taguchi's fractional factorial with 18 trial orthogonal arrays (L_{18}) to investigate the effects of silicon, graphite and tungsten powder mixed with dielectric fluid and other process parameters on the coated surface of a die steel workpiece. Singh *et al* [25] used Taguchi L_{18} ($2^1 \times 3^7$) orthogonal array to investigate the effect of graphite-powder-mixed EDM oil on the surface properties of a superalloy Super Co 605 workpiece.

Although some studies have attempted to optimise EDC parameters, to the best of the authors' knowledge, no study has examined the optimal conditions for the EDC process with recycled quarry dust suspension and the control factors (I_p and T_{on}) for the surface modification of WC–Co. This recycled quarry dust, which is high in SiO_2 and Al_2O_3, is a promising economical alternative to expensive conventional ceramic particles for the surface modification of WC–Co. Therefore, in this study, the optimisation of EDC parameters (I_p and T_{on}) on the characteristics of the coating surface, including its Vickers micro-hardness, surface roughness and coating layer thickness were investigated. Two parameters (I_p and T_{on}) were selected because the coating surface quality is highly depends on the discharge energy which controlled by I_p and T_{on} [26–28]. The response surface methodology (RSM) was applied to generate the parameters matrix, and the optimum EDC parameters were determined and validated at the end of this study.

2. Methodology

2.1. Equipment, materials and experimental condition

A Sodick AQ35L die-sinker EDM machine with 6 mm copper electrode was used in the EDC process. A WC–Co plate of 25 mm $\times$ 25 mm $\times$ 5 mm was chosen as the workpiece material. Table 1 and figure 1 present the element composition and EDX spectrum analysis of the WC–Co workpiece, respectively. Quarry dust powder with an average particle size of 48.423 μm was collected from the Department of Mineral and Geoscience Malaysia. Before the EDC process, quarry dust was mixed with kerosene oil by using a Labsonic ultrasonic homogeniser type P series. A surfactant of Span 85 was then added to the mixture to prevent the agglomeration and sedimentation of quarry dust during the EDC process. Table 2 and table 3 list the elements contained in the quarry dust powder and the conditions for the EDC experiment, respectively, whereas figure 2 presents the *in situ* schematic diagram and photograph image of the experimental setup. The experiments were conducted with reverse polarity where the Cu electrode and WC–Co workpiece were connected to the positive and negative terminals of the power supply, respectively. It was selected to reduce the discharge density at workpiece surface
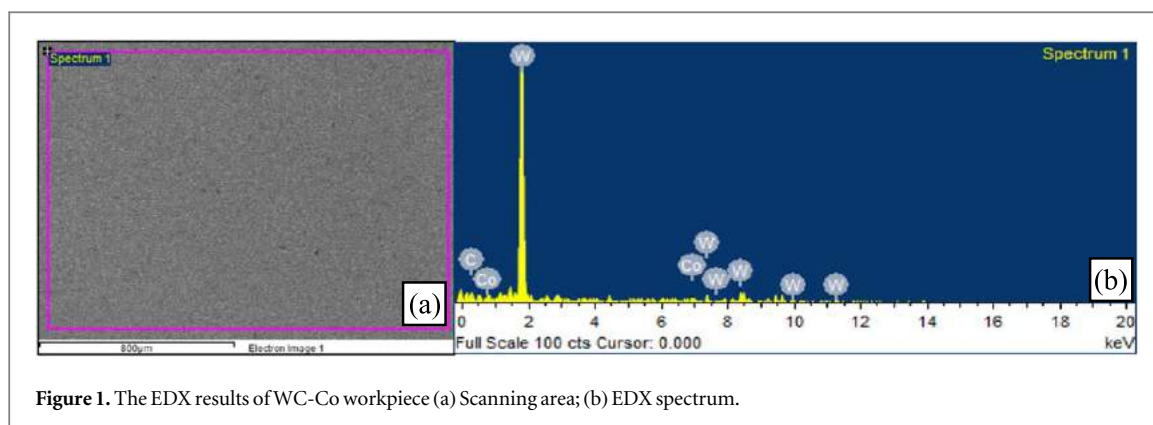
Figure 1. The EDX results of WC-Co workpiece (a) Scanning area; (b) EDX spectrum.

Table 1. The elements weight percentage (%) of WC-Co workpiece.

Elements	Weight Percentage (wt%)
Tungsten (W)	78.98
Carbon (C)	12.99
Cobalt (Co)	8.03

Table 2. Elements content of quarry dust powder (mass %).

Element	Si	Na	Al	K	Fe	Ca	Mg	Ti	Zn	Co	Cr	Rb
Percentage (mass %)	54.0	22.5	10.3	7.0	2.4	1.5	1.3	0.4	0.3	0.1	0.1	0.1

Table 3. Experimental conditions.

Experimental condition	Description
Dielectric fluid	EDM LS (low smell) kerosene oil
The polarity (Reverse polarity)	WC-Co workpiece- negative; Cu electrode-positive
Machining time	30 min
Quarry dust concentration	20 g l^{-1}
Constant/Fixed EDC parameters	
Pulse off tome (T_{off})	30 μs
Discharge voltage (V_d)	40 V

which is a favourable condition for the coating process [29]. A flushing system was also established to circulate the suspended quarry dust in the dielectric fluid during the EDC process.

2.2. Response surface methodology (RSM)
RSM matrix was created in Minitab software to investigate the effects of I_p and T_{on} at two levels and to determine the optimal condition for the EDC process. The adopted design has 27 runs, including 3 replications and central point. Table 4 the EDC parameters and the corresponding levels used in this study.

Vickers micro-hardness, surface roughness and coating layer thickness were used as response variables. Statistical analysis was performed to determine the relationship between the EDC parameters and the responses. Validation tests were performed at the end of the study.

2.3. Measurement and analysis
After the EDC process, an EMAX x-act Energy Dispersive X-ray (EDX) and the X-ray diffraction (XRD) model PANalytical X'Pert Pro MPD were used to determine the weight percentage of elements and components that were deposited on the coating layer. A Mitutoyo HM-210/220 Series 810 micro Vickers hardness testing
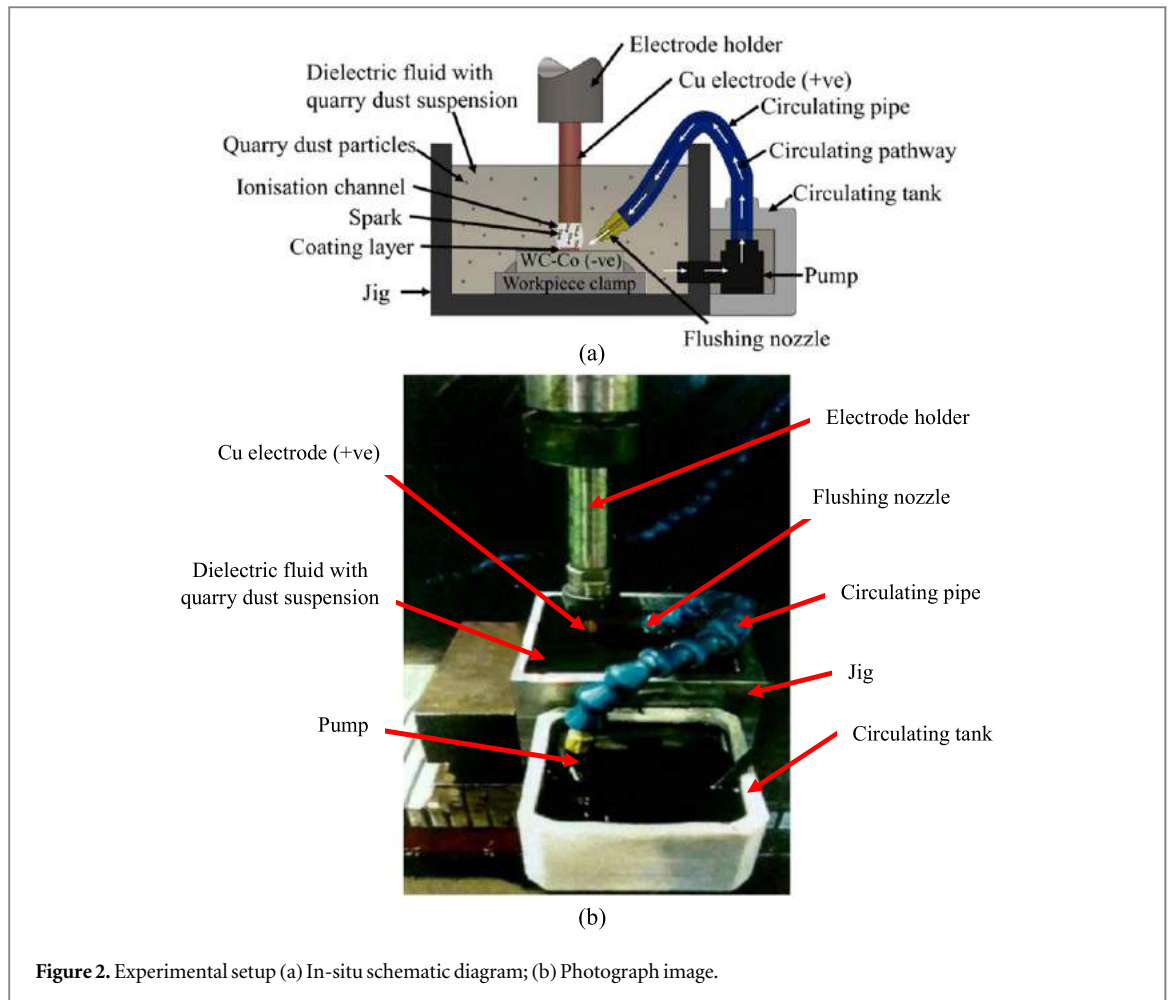
Figure 2. Experimental setup (a) In-situ schematic diagram; (b) Photograph image.

Table 4. The EDC parameters and corresponding level.

EDC parameters	Values	
	Low	High
Peak current (I_p)	3 A	5 A
Pulse on time (T_{on})	100 μs	300 μs

machine was also used to measure the microhardness of the coated surface. The measurements were performed by using a pyramidal indenter with 20 N load and 15 s dwell time. A Mitutoyo SJ-301 portable surface roughness testing machine was also used to measure the roughness of the coated surface. The coated samples were then cut into half by using a Micracut 151 low speed precision cut off machine and were polished by using a diamond abrasive grinding disc in order to obtain the cross section of each sample. A Zeiss EVO 50 scanning electron microscope (SEM) with 4000 $\times$ magnification was used to measure the coating layer thickness. The measurement was repeated 10 times at different spots of the coating layer to ensure data accuracy. The average coating layer thickness was then calculated and recorded in the RSM matrix.

3. Results and discussion

3.1. Coating elements and components

Figure 3 and table 5 present the EDX spectrum analysis and element composition of the coating layer, respectively. A total of nine elements were deposited or coated on the WC–Co surface, namely, carbon (C), magnesium (Mg), aluminium (Al), oxygen (O), silicon (Si), calcium (Ca), zinc (Zn), iron (Fe) and cobalt (Co). C had the highest weight percentage value, followed by Co, Si, Al, Fe, Mg, Ca, Zn and O.

The C elements were released from the decomposition of kerosene oil at high temperature and were deposited on the WC–Co surface during the EDC process following the idea of Collins [30], who argued that
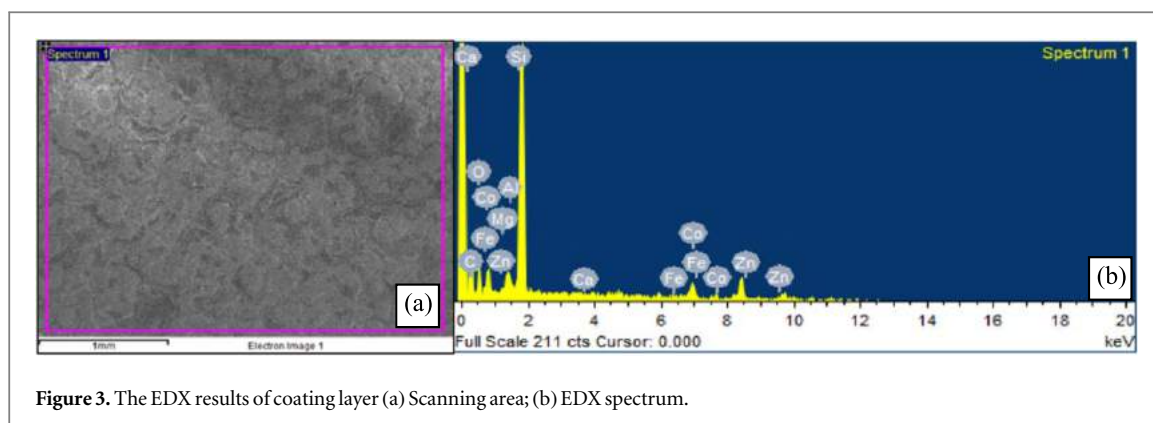
Figure 3. The EDX results of coating layer (a) Scanning area; (b) EDX spectrum.

Table 5. The elements weight percentage (%) of coating layer.

Elements	Weight Percentage (wt%)
Carbon (C)	67.32
Oxygen (O)	0.16
Magnesium (Mg)	3.56
Aluminum (Al)	4.83
Silicon (Si)	5.83
Calcium (Ca)	2.16
Zinc (Zn)	0.69
Iron (Fe)	4.02
Cobalt (Co)	11.43

kerosene oil contains a long hydrocarbon chain of C6 to C16 and a boiling point ranging from 150 °C to 300 °C. However, the EDM die-sinker will generate a spark temperature in the 8000 °C to 12000 °C range between the electrode and workpiece which was highlighted by Abdulkareem *et al* [31]. Therefore, the hydrocarbon chain of kerosene oil was decomposed after the process temperature reached the boiling point of C elements in the plasma channel, thereby resulting in the deposition of carbon particles on the workpiece.

Co, Si, Al, Fe, Mg, Ca and Zn, which were melted from the quarry dust during the EDC process, were also detected on the coated surface. O elements were also detected by the EDX spectrum as part of the coating layer. According to Wang *et al* [32], O will be absorbed by the deposited layer during the cooling process upon its exposure to the atmosphere after EDC.

XRD was used to determine the possible compound or combination of elements in the coating layer. The XRD spectrum graph shown in figure 4 reveals that the coating layer mainly comprises hard carbides and oxide phases (SiC, Mg_2C_3, Fe_2C, SiO_2, Al_2O_3, Fe_2O_3, CaO, CoO, CaC_2 and ZnO) and that SiC has a major diffraction background peak at 2θ/degree angles of 34.2°, 35.5°, 42.5°, 65° and 74.5°. Si, Al, Mg, Ca and Fe were melted from the quarry dust during the EDC process. C was also decomposed from the long carbon chain of kerosene oil and reacted with the Si, Fe, Mg and Ca to form SiC, Fe_2C, Mg_2C_3 and CaC_2, respectively. The oxides of Si, Al, Fe, Zn, Co and Ca were formed during the cooling process when the samples were exposed to the atmosphere after EDC.

3.2. RSM matrix for EDC experiment
Table 6 shows the RSM matrix, including the factors (I_p and T_{on}), response surface roughness, Vickers micro-hardness and coating layer thickness which obtained from EDC process. The ANOVA and response surface plots for these results are discussed in detail in sections 3.3 to 3.5. The level of statistical significance was set to a P-Value of 0.05. The insignificant terms in ANOVA were removed for all responses.

3.3. Surface roughness
Table 7 presents the ANOVA results for surface roughness. The insignificance of 'Lack-of-Fit' suggests that the proposed model has good fit to the average surface roughness data. Figure 5 shows the response surface plot for surface roughness. I_p has a higher inclination line than T_{on}, which agrees with the results shown in table 7 because the F-Value of I_p (623.98) is higher than that of T_{on} (236.02). Therefore, I_p is the most statistically significant parameter of surface roughness. Figure 5 shows that the average surface roughness significantly
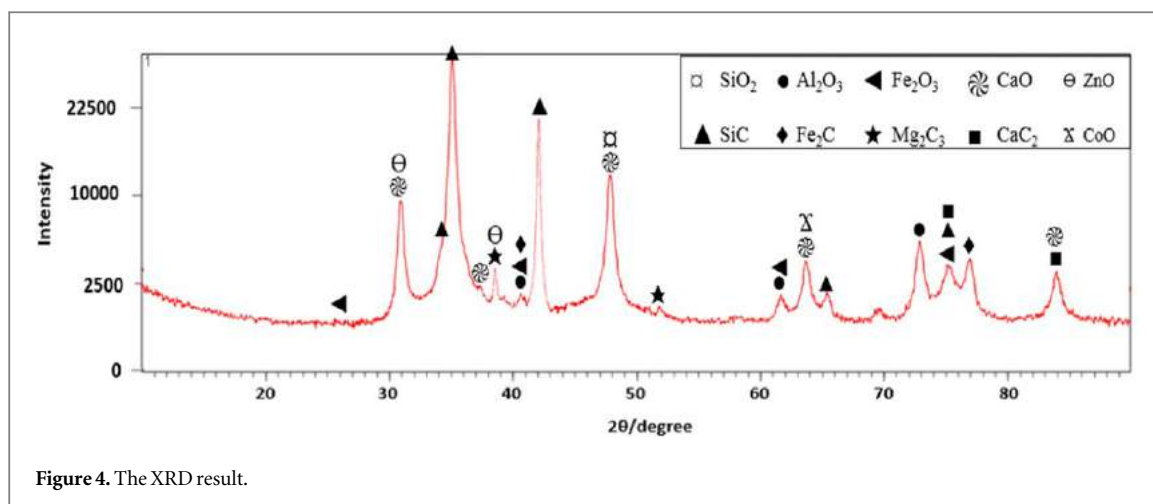
Figure 4. The XRD result.

Table 6. RSM matrix.

		Factor		Response		
Std Order	Run Order	I_p (A)	T_{on} (μs)	Surface Roughness (μm)	Vickers Micro-Hardness (HV)	Coating Layer Thickness (μm)
2	1	5.00	100	4.11	1736.03	4.428
8	2	4.00	341	4.82	1838.24	5.992
13	3	5.00	300	5.04	1870.29	6.330
1	4	3.00	100	2.69	1665.00	2.105
22	5	5.00	300	5.27	1873.63	6.283
3	6	3.00	300	3.52	1760.53	4.805
5	7	2.59	200	3.03	1674.98	3.243
18	8	4.00	200	4.10	1768.31	4.168
17	9	4.00	341	4.48	1858.32	5.801
26	10	4.00	341	4.64	1837.52	5.674
7	11	4.00	59	3.11	1674.39	2.848
27	12	4.00	200	3.87	1743.27	3.191
24	13	5.41	200	5.05	1812.44	5.306
14	14	2.59	200	2.83	1728.56	2.799
9	15	4.00	200	4.22	1763.19	3.679
6	16	5.41	200	4.87	1836.89	5.259
25	17	4.00	59	3.31	1697.91	2.785
20	18	5.00	100	4.28	1752.86	4.331
19	19	3.00	100	2.75	1647.11	2.085
4	20	5.00	300	5.46	1847.79	6.466
21	21	3.00	300	3.71	1781.94	4.216
16	22	4.00	59	3.51	1669.11	2.754
15	23	5.41	200	5.23	1812.47	5.096
23	24	2.59	200	2.66	1682.45	3.223
10	25	3.00	100	2.42	1671.72	2.251
12	26	3.00	300	3.65	1787.36	4.683
11	27	5.00	100	4.31	1762.70	4.199

increases when the peak current increases from 3 A to 5 A. This relationship can be explained by the increase in the discharge energy and spark amount (the amount of spark generated during an on-time). Specifically, the discharge energy and spark amount increase after applying a high I_p during the EDC process, which leads to a non-uniform or irregular coating on the surface of the WC–Co workpiece and subsequently results in a high surface roughness. This result is consistent with those of Rahang and Patowari [21], who reported the lowest and highest surface roughness values is found at 3 A and 6 A of I_p, respectively. Surface roughness also increased along with T_{on}, probably due to the deposition of additional quarry dust powder on the surface of the WC–Co workpiece along with an increasing T_{on}. The migration of quarry dust powder into the ionisation channel also increased along with T_{on}, which resulted in the direct deposition or trapping of unmelted quarry dust particles in the melted section of the workpiece surface, thereby increasing surface roughness. Equation (1) presents the
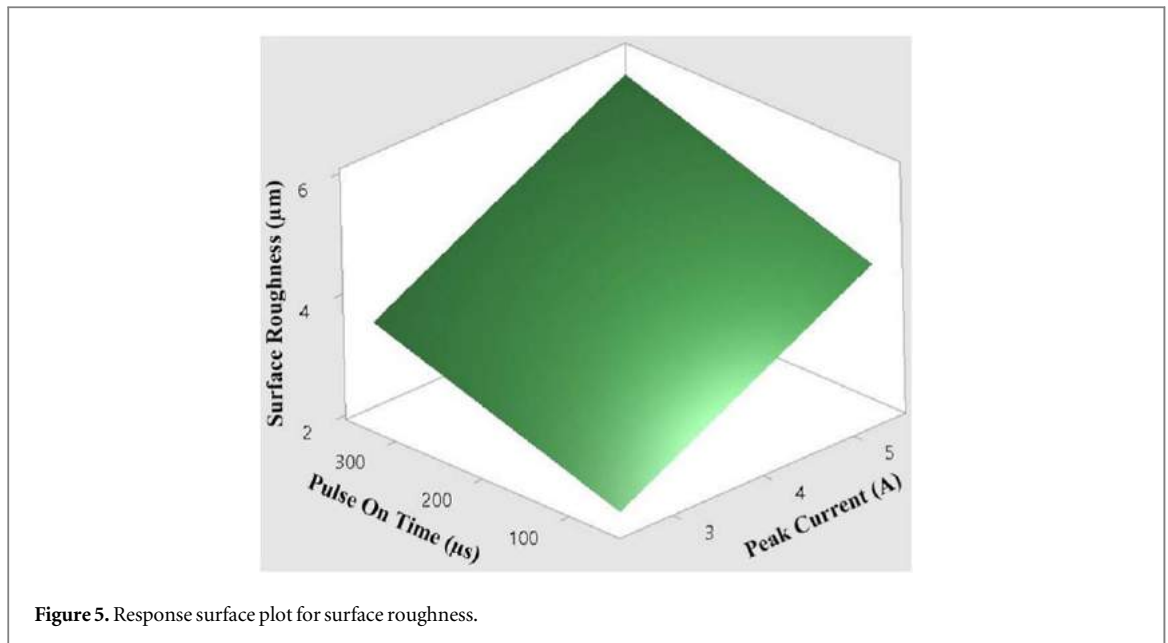
Figure 5. Response surface plot for surface roughness.

Table 7. ANOVA for surface roughness.

Source	DF	Adj SS	Adj MS	F-Value	P-Value	Remark
Model	2	20.9554	10.4777	430.00	<0.0001	Significant
Linear	2	20.9554	10.4777	430.00	<0.0001	Significant
Peak Current	1	15.2044	15.2044	623.98	<0.0001	Significant
Pulse on Time	1	5.7510	5.7510	236.02	<0.0001	Significant
Error	24	0.5848	0.0244			
Lack-of-Fit	6	0.0547	0.0091	0.31	0.9236	Not significant
Pure Error	18	0.5301	0.0294			
Total	26	21.5402				

Table 8. ANOVA for Vickers micro-hardness.

Source	DF	Adj SS	Adj MS	F-Value	P-Value	Remark
Model	2	20.9554	10.4777	430.00	<0.0001	Significant
Linear	2	20.9554	10.4777	430.00	<0.0001	Significant
Peak Current	1	15.2044	15.2044	623.98	<0.0001	Significant
Pulse on Time	1	5.7510	5.7510	236.02	<0.0001	Significant
Error	24	0.5848	0.0244			
Lack-of-Fit	6	0.0547	0.0091	0.31	0.9236	Not significant
Pure Error	18	0.5301	0.0294			
Total	26	21.5402				

regression equation for surface roughness response.

$$\text{Surface roughness } (\mu m) = -0.209$$
$$+ \ 0.7971 \text{ Peak Current}$$
$$+ \ 0.004902 \text{ Pulse on Time} \tag{1}$$

3.4. Vickers micro-hardness

Table 8 presents the ANOVA results for Vickers micro-hardness. The 'Lack-of-Fit' (P-Value $= 0.9957$) was insignificant relative to the pure error given that the P-Value was greater than 0.05, thereby suggesting that this model has good fit to the average Vickers micro-hardness data.

Figure 6 shows the response surface plot for Vickers micro-hardness. T_{on} has a higher inclination line than I_p, which is consistent with the results presented in table 8 given that the F-Value of T_{on} (396.8530) is higher than
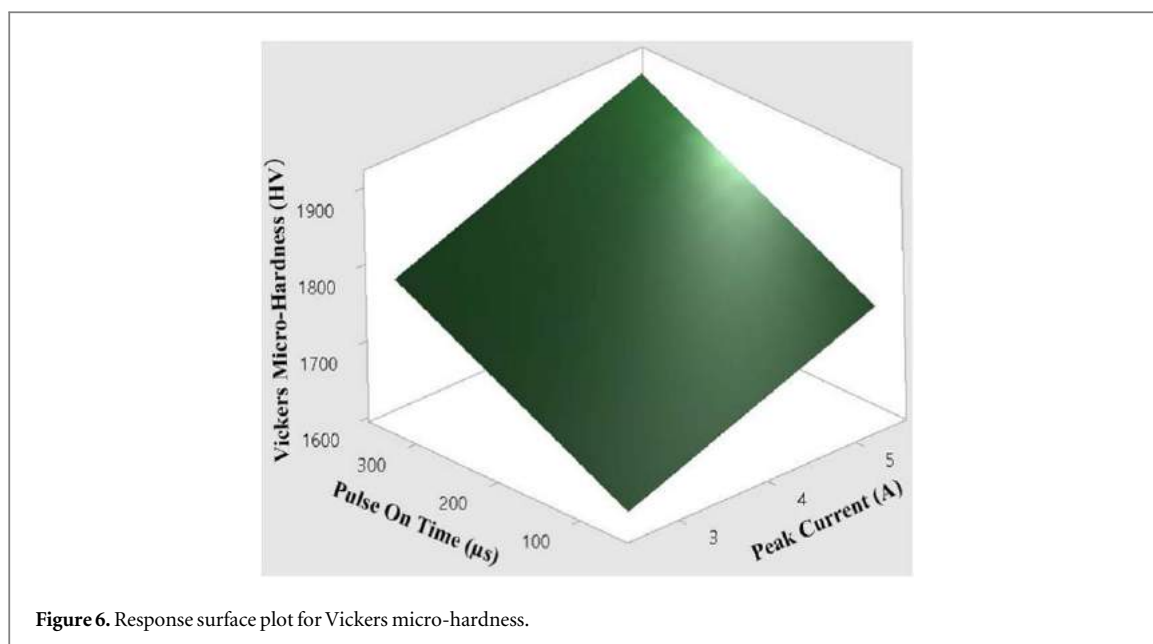
Figure 6. Response surface plot for Vickers micro-hardness.

that of I_p (233.6676). Therefore, T_{on} is the most statistically significant parameter of Vickers micro-hardness. As shown in figure 6, the average Vickers micro-hardness significantly increases as T_{on} increases from 100 μs to 300 μs. However, the average Vickers micro-hardness only moderately increases when I_p increases from 3 A to 5 A. These phenomena can be explained by discharge energy, which refers to the mean value of electrical energy per impulse that is transformed into thermal energy in the EDM process. The discharge energy is influenced by I_p and T_{on} [33]. Increasing these parameters will also increase the discharge energy and lead to the transformation of additional electrical energy into thermal energy in the discharge zone. Consequently, a large amount of quarry dust will be melted and coated on the WC–Co workpiece surface, thereby increasing micro-hardness.

An increment in micro-hardness may also be ascribed to the formation of SiC in the XRD analysis as shown in figure 4. The formation of SiC is related to the chemical reaction between Si (main element of quarry dust) and C that may be decomposed from kerosene oil. The synthesis of SiC may result from carbothermic reduction. According to Dijen and Metselaar [34], SiC is produced at temperatures ranging from 1400 °C to 2400 °C. Given the extremely high discharge temperature (8000 °C–12000 °C) during the EDC process, SiC was easily formed and deposited on the workpiece surface. Equation (2) presents the regression equation of Vickers micro-hardness.

$$
\begin{aligned}
\text{Vickers micro} - \text{hardness (HV)} &= 1468.8 \\
&+ 44.28 \text{ Peak Current} \\
&+ 0.5770 \text{ Pulse on Time}
\end{aligned}
\tag{2}
$$

3.5. Coating Layer Thickness

Table 9 shows that 'Lack-of-Fit' has a P-Value of 0.0769, which exceeds the statistically significant level of 0.05, thereby suggesting that the model has good fit to the coating layer thickness data.

Figure 7 presents the response surface plot for coating layer thickness. The coating layer thickness possessed an exponential growth to both the I_p and T_{on}. However, the inclination line and F-Value of T_{on} are greater than those of I_p, thereby suggesting that T_{on} is the most significant parameter for coating layer thickness. This result is likely to be related to the study in Subtopic 3.3 of surface roughness where this situation occurred due to the strong discharge energy caused by the rising of I_p and T_{on}. Therefore, the melting of additional quarry dust and the decomposition of kerosene oil to release C elements that are deposited on the workpiece surface may result in higher coating layer thickness. These results agree with those of Chen *et al* [35]. Equation (3) presents the mathematical model for coating layer thickness. Table 10 presents the SEM images of average coating layer thickness for different I_p and T_{on}. As shown in this table, the coating layer thickness significantly increases along with I_p and T_{on}.
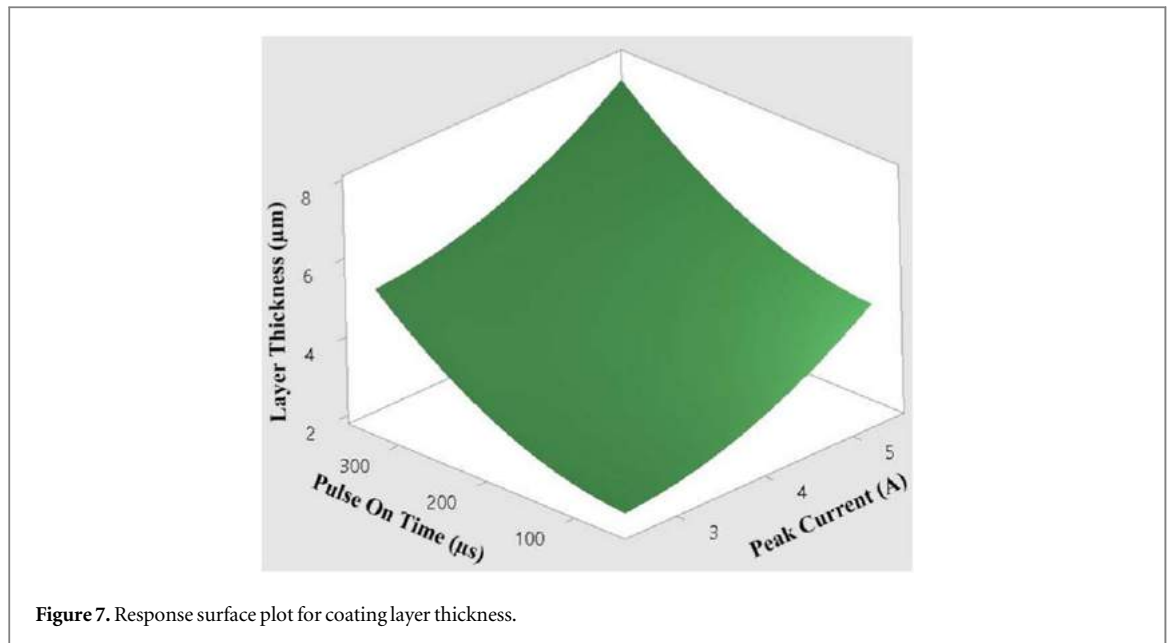
Figure 7. Response surface plot for coating layer thickness.

Table 9. ANOVA for coating layer thickness.

Source	DF	Adj SS	Adj MS	F-Value	P-Value	Remark
Model	4	48.0068	12.0017	180.546	< 0.0001	Significant
Linear	2	46.935	23.4675	353.029	< 0.0001	Significant
Peak Current	1	18.2747	18.2747	274.913	< 0.0001	Significant
Pulse on Time	1	28.6603	28.6603	431.146	< 0.0001	Significant
Square	2	1.0718	0.5359	8.062	0.0024	Significant
Peak Current*Peak Current	1	0.6233	0.6233	9.376	0.0057	Significant
Pulse on Time*Pulse on Time	1	1.0375	1.0375	15.607	0.0007	Significant
Error	22	1.4624	0.0665			
Lack-of-Fit	4	0.5257	0.1314	2.525	0.0769	Not significant
Pure Error	18	0.9367	0.052			
Total	26	49.4692				

$$
\begin{aligned}
\text{Coating layer thickness}(\mu\text{m}) \\
= 3.67 - 1.271 \text{ Peak Current} \\
+ 0.00290 \text{ Pulse on Time} \\
+ 0.2682 \text{ Peak Current} \\
* \text{ Peak Current} + 0.000035 \text{ Pulse on Time} \\
* \text{Pulse on Time}
\end{aligned}
\tag{3}
$$

3.6. Optimum parameter and validation test

Table 11 shows the optimisation goal for the optimum parameters I_p and T_{on}. Surface roughness, Vickers micro-hardness and coating layer thickness were used as the criteria for obtaining the optimum parameters. Table 12 shows the optimum parameters selected by the software based on the above criteria. The optimum parameters are $I_p = 4$ A and $T_{on} = 341 \ \mu$s.

As mentioned in section 1, WC–Co is widely used in many industrial applications, including as cutting tools, dies and moulds. Therefore, maximum hardness, minimum surface roughness and maximum coating layer thickness are necessary to extend the service life of WC–Co. High hardness and coating layer thickness are also important to protect the WC–Co surface from wear and corrosion.

A validation test was performed to determine the accuracy of all models developed in this research. A set of random parameters was chosen (not listed in the RSM matrix) for the validation. The randomly chosen parameters were $I_p = 5$ A and $T_{on} = 200 \ \mu$s. Table 13 presents the validation experiment results.

The validation test errors for Vickers micro-hardness, surface roughness and coating layer thickness were 0.1694%, 1.5303% and 0.7427%, respectively. With the confidence level set at 95%, all errors that do not exceed 5% were considered fit. Therefore, all RSM models developed in this study were deemed accurate and valid.

Table 10. Average coating layer thickness by using different I_p and T_{on}

Average Coating Thickness: 3.243 μm

WC-Co workpiece

5 μm
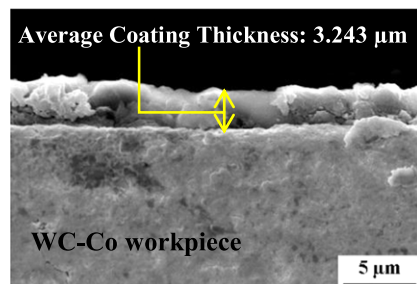
Parameters: $I_p = 2.59$ A, $T_{on} = 200$ μs

Average Coating Thickness: 5.259 μm

WC-Co workpiece

5 μm
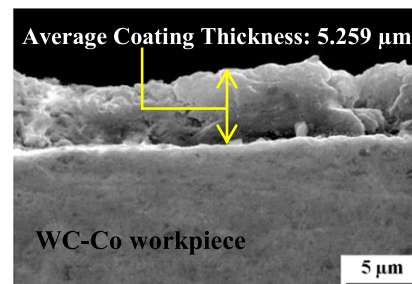
Parameters: $I_p = 5.41$ A, $T_{on} = 200$ μs
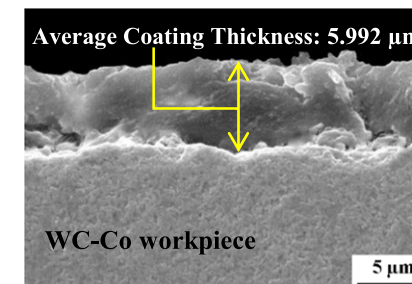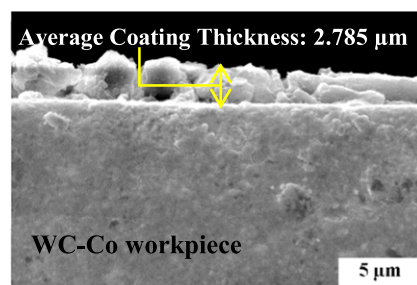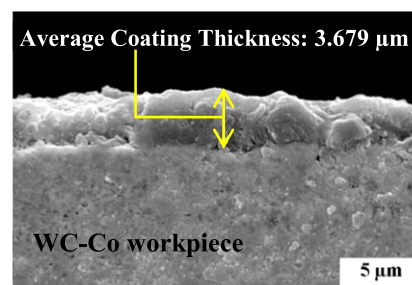
Average Coating Thickness: 5.992 μm

WC-Co workpiece

5 μm

Parameters: $I_p = 4$ A, $T_{on} = 341$ μs

Average Coating Thickness: 2.785 μm

WC-Co workpiece

5 μm

Parameters: $I_p = 4$ A, $T_{on} = 59$ μs

Average Coating Thickness: 3.679 μm

WC-Co workpiece

5 μm

Parameters: $I_p = 4$ A, $T_{on} = 200$ μs

Average Coating Thickness: 2.251 μm

WC-Co workpiece

5 μm

Parameters: $I_p = 3$ A, $T_{on} = 100$ μs

Average Coating Thickness: 4.216 μm

WC-Co workpiece

5 μm

Parameters: $I_p = 3$ A, $T_{on} = 300$ μs

Average Coating Thickness: 4.199 μm

WC-Co workpiece

5 μm

Parameters: $I_p = 5$ A, $T_{on} = 100$ μs

Average Coating Thickness: 6.466 μm

WC-Co workpiece

5 μm
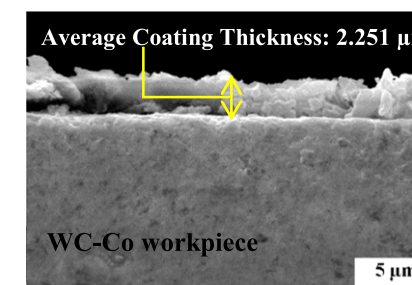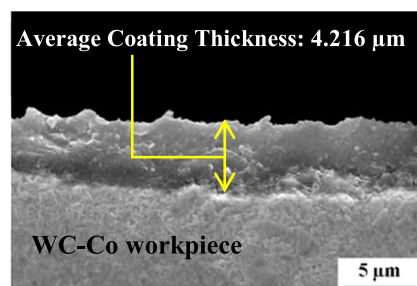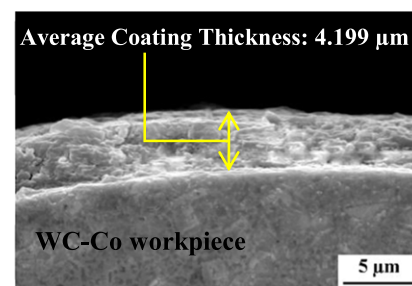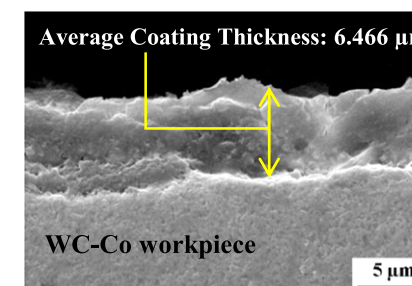
Parameters: $I_p = 5$ A, $T_{on} = 300$ μs

Table 11. Optimisation goal for the optimum parameters.

Response	Goal	Lower limit	Upper limit
Vickers micro-hardness (HV)	Maximum	1647.11	1873.63
Surface roughness (μm)	Minimum	2.42	5.46
Coating layer thickness (μm)	Maximum	2.085	6.466

Table 12. Optimum parameters.

Parameters	Optimum value
I_p	4 A
T_{on}	341 μs

Table 13. Result of the validation experiment.

	Random parameters					
	$I_p = 5$ A and $T_{on} = 200$ μs					
		Experimental result				
		Replication				
Responses	Predicted result	1	2	3	Average	Error (%)
Vickers micro-hardness	1805.5747 HV	1807.30 HV	1803.30 HV	1815.30 HV	1808.63 HV	0.1694
Surface roughness	4.7572 μm	4.88 μm	4.85 μm	4.76 μm	4.83 μm	1.5303
Layer thickness	4.8517 μm	4.9014 μm	4.8534 μm	4.8126 μm	4.8558 μm	0.7427

4. Conclusions

This study focuses on the optimisation of EDC parameters with quarry dust suspension by using RSM. The effects of EDC parameters I_p and T_{on} on the Vickers micro-hardness, surface roughness and coating layer thickness were also investigated. The following points can be drawn from the findings:

1. Quarry dust powder can be used as an eco-friendly alternative material for surface modification of WC–Co workpiece.

2. Increasing both I_p and T_{on} will also increase the Vickers micro-hardness and coating layer thickness yet decrease the surface finish of the coated layer.

3. The optimum parameters necessary to achieve a hard and thick coating layer with a low surface roughness value were $I_p = 4$ A and $T_{on} = 341$ μs.

4. After the EDC process, the migration of materials from the quarry dust powder and dielectric fluid resulted in the growth of the coating layer on the WC–Co workpiece. The formation of hard carbides, especially SiC, on the coating layer enhanced the micro-hardness of the WC–Co workpiece.

Acknowledgments

Conflict of Interests

The authors declare that there is no conflict of interest regarding the publication of this paper.

ORCID iDs

Ching Yee Yap ⓘ https://orcid.org/0000-0002-8919-7676
Pay Jun Liew ⓘ https://orcid.org/0000-0001-6729-1576

References

[1] Gee M G, Gant A and Roebuck B 2007 Wear mechanisms in abrasion and erosion of WC/Co and related hardmetals *Wear* **263** 137–48

[2] Ma R, Ju S, Chen H and Shu C 2017 Effect of cobalt content on microstructures and wear resistance of tungsten carbide–cobalt-cemented carbides fabricated by spark plasma sintering *IOP Conf. Ser.: Mater. Sci. Eng.* **207** 012019

[3] Janmanee P and Muttamara A 2012 Surface modification of tungsten carbide by electrical discharge coating (EDC) using a titanium powder suspension *Appl. Surf. Sci.* **258** 7255–65

[4] Chakraborty S, Kar S, Dey V and Ghosh S K 2017 The phenomenon of surface modification by electro-discharge coating process: a review *Surf. Rev. Lett.* **25** 1830003

[5] Liew P J, Yap C Y, Wang J, Zhou T and Yan J 2020 Surface modification and functionalization by electrical discharge coating: a comprehensive review *Int. J. Extrem. Manuf.* **2** 012004

[6] Hwang Y, Kuo C and Hwang S 2010 The coating of TiC layer on the surface of nickel by electric discharge coating (EDC) with a multi-layer electrode *J. Mater. Process. Technol.* **210** 642–52

[7] Molinetti A, Amorim F L, Soares P C and Czelusniak T 2016 Surface modification of AISI H13 tool steel with silicon or manganese powders mixed to the dielectric in electrical discharge machining process *Int. J. Adv. Manuf. Technol.* **83** 1057–68

[8] Liew P J, Yap C Y, Nurlishafiqa Z, Othman I S, Chang S Y, Toibah A R and Wang J 2018 Material deposition on aluminium by electrical discharge coating (EDC) with a tungsten powder suspension *J. Adv. Manuf. Technol* **12** 133–46

[9] Elaiyarasan U, Satheeshkumar V and Senthilkumar C 2018 Experimental analysis of electrical discharge coating characteristics of magnesium alloy using response surface methodology *Mater. Res. Express* **5** 086501

[10] Arun I, Gangadhar B, Yuvaraj C and Kousalya C 2019 Electrical discharge metal matrix composite coating on duplex stainless steel and its wear behavior under different environmental conditions *Mater. Res. Express* **6** 0965c5

[11] Rao P S, Purnima N S and Prasad D S 2018 Surface alloying of D2 steel using EDM with WC/Co P/M electrodes made of Nano and Micron sized particles *Mater. Res. Express* **6** 036511

[12] Chen H J, Wu K L and Yan B H 2014 Characteristics of Al alloy surface after EDC with sintered Ti electrode and TiN powder additive *Int. J. Adv. Manuf. Technol.* **72** 319–32

[13] Sharma D, Mohanty S and Das A K 2020 Surface modification of titanium alloy using hBN powder mixed dielectric through micro-electric discharge machining *Surf. Coatings Technol.* **381** 125157

[14] Mohanty S, Kumar V, Kumar Das A and Dixit A R 2019 Surface modification of Ti-alloy by micro-electrical discharge process using tungsten disulphide powder suspension *J. Manuf. Process.* **37** 28–41

[15] Mansor A F, Azmi A I, Zain M Z M and Jamaluddin R 2020 Parametric evaluation of electrical discharge coatings on nickel-titanium shape memory alloy in deionized water *Heliyon.* **6** e04812

[16] Tyagi R, Das A K and Mandal A 2018 Electrical discharge coating using WS2 and Cu powder mixture for solid lubrication and enhanced tribological performance *Tribol. Int.* **120** 80–92

[17] Philip J T, Kumar D, Mathew J and Kuriachen B 2020 Tribological investigations of wear resistant layers developed through EDA and WEDA techniques on Ti6Al4V surfaces: Part I—Ambient temperature *Wear* **458–459** 203409

[18] Philip J T, Kumar D, Mathew J and Kuriachen B 2020 Experimental Investigations on the Tribological Performance of Electric Discharge Alloyed Ti–6Al–4V at 200–600 °C *J. Tribol.* **142** 061702

[19] Yu Y T, Hsieh S F, Lin M H, Huang J W and Ou S-F 2020 Improvement in Ca and P incorporation in the coating on Ti by gas-assisted electrical discharge coating *Surf. Coatings Technol.* **400** 126120

[20] Marashi H, Jafarlou D M, Sarhan A A D and Hamdi M 2016 State of the art in powder mixed dielectric for EDM applications *Precis. Eng.* **46** 11–33

[21] Rahang M and Patowari P K 2016 Parametric optimization for selective surface modification in EDM using taguchi analysis *Mater. Manuf. Process.* **31** 422–31

[22] Chakraborty S, Kar S, Dey V and Ghosh S K 2017 Optimization and surface modification of Al-6351 alloy using SiC–Cu green compact electrode by electro discharge coating process *Surf. Rev. Lett.* **24** 1750007

[23] Vijayakumar S, Mohan N, Dineshbabu C and Karthikeyan G 2016 Reduce the mass losses for coated Al 7075 by using powder mixed electric discharge coating *Int. J. Mod. Trends Eng. Sci.* **3** 184–6

[24] Bhattacharya A, Batish A and Kumar N 2013 Surface characterization and material migration during surface modification of die steels with silicon, graphite and tungsten powder in EDM process *J. Mech. Sci. Technol.* **27** 133–40

[25] Singh A K, Kumar S and Singh V P 2015 Effect of the addition of conductive powder in dielectric on the surface properties of superalloy Super Co 605 by EDM process *Int. J. Adv. Manuf. Technol.* **77** 99–106

[26] Prakash C, Kansal H K, Pabla B S and Puri S 2017 Experimental investigations in powder mixed electric discharge machining of Ti–35Nb–7Ta–5Zrβ-titanium alloy *Mater. Manuf. Process.* **32** 274–85

[27] Algodi S J, Murray J W, Fay M W, Clare A T and Brown P D 2016 Electrical discharge coating of nanostructured TiC-Fe cermets on 304 stainless steel *Surf. Coatings Technol.* **307** 639–49

[28] Prakash C, Singh S, Pruncu C, Mishra V, Królczyk G, Pimenov D and Pramanik A 2019 Surface modification of Ti-6Al-4V alloy by electrical discharge coating process using partially sintered Ti-Nb electrode *Materials (Basel)* **12** 1006

[29] Schulze H P 2017 Importance of polarity change in the electrical discharge machining *Proc. 20th Int. ESAFORM Conf. Mater. Form.* (Dublin, Ireland: AIP Publishing) p 050001

[30] Collins C D 2007 *Implementing Phytoremediation of Petroleum Hydrocarbons Phytoremediation* **23** 99–108

[31] Abdulkareem S, Ali Khan A and Konneh M 2010 Cooling effect on electrode and process parameters in EDM *Mater. Manuf. Process.* **25** 462–6

[32] Wang Y K, Wang W M, Cu X H, Cheng X Y, Li B S, Xia L F and Lei T Q 1993 A study of the oxide layer on the surface of a TiN coating *Mater. Chem. Phys.* **36** 80–3

[33] Gostimirovic M, Kovac P, Sekulic M and Skoric B 2012 Influence of discharge energy on machining characteristics in EDM *J. Mech. Sci. Technol.* **26** 173–9

[34] Dijen F K and Metselaar R 1991 The chemistry of the carbothermal synthesis of β-SiC: Reaction mechanism, reaction rate and grain growth *J. Eur. Ceram. Soc.* **7** 177–84

[35] Chen S L, Lin M H, Huang G X and Wang C C 2014 Research of the recast layer on implant surface modified by micro-current electrical discharge machining using deionized water mixed with titanium powder as dielectric solvent *Appl. Surf. Sci.* **311** 47–53